

Optimal Design of Phase Function in Generalized DFT

Ali N. Akansu, Handan Agirman-Tosun and Mustafa U. Torun

New Jersey Institute of Technology

Department of Electrical & Computer Engineering

University Heights, Newark, NJ 07102 USA

Email: Akansu@NJIT.EDU

Tel: (973) 596-5650 Fax: (973) 596-5680

Abstract— Recently, a theoretical framework for Generalized DFT (GDFT) with nonlinear phase functions exploiting the phase space to design various constant modulus orthogonal transforms was introduced. This paper extends prior work to design longer bases widely used in real world communications systems. GDFT provides flexibilities in phase space yielding performance improvements over other code families including DFT in correlation metrics. GDFT phase functions are optimally designed in order to reduce inter carrier interference (ICI) and inter-symbol interference (ISI) that dictate the performance of a multiuser channel. It is presented in the paper that superior correlation of GDFT over DFT manifests itself in improved BER performance in direct sequence CDMA based multi-user communications systems.

Index Terms— Auto-correlation Function, Cross-correlation Function, Discrete Fourier Transform (DFT), Generalized Discrete Fourier Transform (GDFT), Walsh Codes, Gold Codes, Direct Sequence Code Division Multiple Access (DS/CDMA).

I. INTRODUCTION

The most popular multiuser communications systems include time division multiple access (TDMA), frequency division multiple access (FDMA), code division multiple access (CDMA) and orthogonal frequency division multiplexing (OFDM) types. Among them, TDMA employs time-localized orthogonal function sets where the basis functions are all-pass like in frequency-domain. In contrast, in FDMA, carrier functions are localized in frequency-domain and spread in time-domain. In CDMA, code sets are simultaneously spread both in the time-domain and the frequency-domain. In these multiple access techniques, function sets are desired to be orthogonal. Orthogonality in time is required to reduce interference, inter-symbol interference (ISI), between sub-symbols transmitted on the same carrier as in TDMA communications. On the other hand, orthogonality in frequency domain ensures no interference, inter-carrier interference (ICI), among various carriers or sub-channels as in OFDM/FDMA systems. In CDMA applications, orthogonality is in the code domain in order to mitigate multi-user interference (MUI). For the synchronous communications case, code orthogonality is the sufficient property to ensure no interference exists among carriers. In the asynchronous communications scenario, orthogonality is not sufficient to mitigate interference. Hence, correlation properties of orthogonal function set plays crucial role in system performance.

Design of function sets and various orthogonal user codes with desirable time and frequency domain properties has been an active research topic for the last several decades. Among various popular spreading code families, Gold codes [1] have been successfully used in asynchronous direct sequence code division multiple access (DS/CDMA) communications systems due to their low cross-correlation characteristics [2]. Walsh [3], Gold, Walsh-like [4] and several other binary sets are widely employed in practice for various applications. Spreading codes with non-binary real chip values with improved auto- and cross-correlations were also studied in the literature. More recently, research has focused on constant modulus spreading codes due to the limited efficiency of non-linear power amplifiers in radio transceivers. Roots of

unity were utilized in complex spreading codes proposed by several authors in the literature. Frank-Zadoff, Chu (FZC) and Oppermann introduced a variety of such complex spreading codes [5-9]. Moreover, FZC sequences were shown to be the special cases of Oppermann sequences [8, 9].

Discrete Fourier Transform (DFT) has become the most popular orthogonal transform since the introduction of its efficient implementation, namely FFT algorithms. The orthogonality with linear phase, relatively low auto- and cross-correlations, and frequency localized features of basis functions make DFT a natural multiplexing technique for frequency selective communications applications such as OFDM. OFDM is proposed for 4G communications systems due to its spectral efficiency, strong resistance to multipath fading, and implementation efficiency. More recently, the Generalized Discrete Fourier Transform (GDFT) framework with non-linear phase was introduced, and it was shown that widely used orthogonal sets are the special cases of GDFT [10]. Several GDFT designs with short lengths were also presented in [11] and [12]. In this paper, we extend previous GDFT results to longer length codes that find their use in various real world systems. The proposed GDFT framework is employed in the generation of orthogonal function sets with improved correlation properties. These orthogonal codes are employed in a DS/CDMA system with additive white Gaussian noise (AWGN) and Rayleigh channel models. Their superior performance in multi-user communications over known orthogonal code families is presented.

The motivation of work and the GDFT framework is explained in Section II. Several methods to design optimal GDFT with respect to correlation metrics of interest are highlighted in Section III. The BER performance simulation results for a various communications scenarios are displayed in Section IV. The conclusions and future work are discussed in Section V.

II. GENERALIZED DISCRETE FOURIER TRANSFORM

An N^{th} root of unity in the complex plane satisfies the equation

$$z^N = 1 \quad N \in \{1, 2, 3, \dots\} \quad (1)$$

If $z_p^m \neq 1$; $m \in \{1, 2, \dots, N-1\}$, then z_p is defined as the p^{th} primitive N^{th} root of unity and m and N must be coprime integer numbers. The complex number $z_1 = e^{j(2\pi/N)}$ is the primitive N^{th} root of unity with the smallest positive argument. There are N distinct N^{th} roots of unity for any primitive and expressed as

$$z_k = (z_p)^k \quad k = 1, 2, 3, \dots, N \quad (2)$$

where z_p is any of the primitive N^{th} root of unity. All primitive N^{th} roots of unity satisfy the summation property of a geometric series as expressed in

$$\sum_{n=0}^{N-1} (z_p)^n = \frac{(z_p)^N - 1}{z_p - 1} = \begin{cases} 1, & N = 1 \\ 0, & N > 1 \end{cases} \quad \forall p \quad (3)$$

Now, we define a periodic, constant modulus, complex sequence $\{e_r(n)\}$ as the r^{th} power of the first primitive N^{th} root of unity z_1 raised to the n^{th} power as defined

$$e_r(n) \triangleq (z_1^r)^n = e^{j(2\pi r/N)n} \quad (4)$$

$n = 0, 1, 2, \dots, N-1$ and $r = 0, 1, 2, \dots, N-1$

The complex sequence of (4) over a finite discrete-time interval in a geometric series is expressed according to (3) as follows [13, 14],

$$\frac{1}{N} \sum_{n=0}^{N-1} e_r(n) = \frac{1}{N} \sum_{n=0}^{N-1} e^{j(2\pi r/N)n} = \begin{cases} 1, & r = mN \\ 0, & r \neq mN \\ & m = \text{integer} \end{cases} \quad (5)$$

Then, we rewrite (5) as the discrete Fourier transform (DFT) set $\{e_k(n)\}$ satisfying the orthonormality conditions [15]

$$\langle e_k(n), e_l^*(n) \rangle = \frac{1}{N} \sum_{n=0}^{N-1} e^{j(2\pi/N)(k-l)n} = \begin{cases} 1, & r = k - l = mN \\ 0, & r = k - l \neq mN \\ & m = \text{integer} \end{cases} \quad (6)$$

The notation (*) indicates the conjugate function of a complex function. The first primitive N^{th} root of unity was shown above as $z_1 = e^{j\omega_0}$ where $\omega_0 = 2\pi/N$ in radians, and called *the fundamental frequency*. We extend the phase functions of (6) in order to express the nonlinear phase GDFT as follows.

Let's rewrite the phase in (5) as the difference of two functions $\varphi_{kl}(n) = \varphi_k(n) - \varphi_l(n) = r$. Then, a constant modulus orthogonal set might be defined as follows [10-12],

$$\frac{1}{N} \sum_{n=0}^{N-1} e^{j[2\pi\varphi_{kl}(n)/N]n} = \begin{cases} 1, & \varphi_{kl}(n) = \varphi_k(n) - \varphi_l(n) = k - l = r = mN \\ 0, & \varphi_{kl}(n) = \varphi_k(n) - \varphi_l(n) = k - l = r \neq mN \\ & m = \text{integer } 0 \leq k, l, n \leq N - 1 \end{cases} \quad (7)$$

By inspection,

$$\langle e_k(n), e_l^*(n) \rangle = \frac{1}{N} \sum_{n=0}^{N-1} e^{j[2\pi(\varphi_k(n) - \varphi_l(n))/N]n} \quad (8)$$

Hence, the transform kernel is defined as [10]

$$\{e_k(n)\} \triangleq e^{j(2\pi/N)\varphi_k(n)n} \quad k, n = 0, 1, \dots, N - 1 \quad (9)$$

This orthogonal set is called the *Generalized Discrete Fourier Transform* (GDFT). Equations (6) and (7) state that this set is *uncountable*, and there are infinitely many constant modulus sets with *nonlinear and linear phase functions* whereas DFT is the unique set with linear phase for the case of $\varphi_k(n) = k \forall n$.

Therefore, one might methodically design such GDFT sets based on performance metrics of interest.

As one possible design method, we define the discrete time rational function $\varphi_k(n)$ in (8) as,

$$\varphi_k(n) = \frac{N_k(n)}{D_k(n)} = \frac{\sum_{j=1}^N a_{kj} n^{b_{kj}}}{\sum_{j=1}^M c_{kj} n^{d_{kj}}} \quad N \leq M; \quad k \in \{0, 1, \dots, N-1\} \quad (10)$$

Assume that the denominator polynomial $D_k(n) = 1$ and the numerator polynomial is expressed as

$$\varphi_k(n) = N_k(n) = \sum_{j=1}^N a_{kj} n^{b_{kj}} = a_{k1} n^{b_{k1}} + a_{k2} n^{b_{k2}} + a_{k3} n^{b_{k3}} + \dots + a_{kN} n^{b_{kN}} \quad (11)$$

The polynomial coefficients $\{a_{kj}\}$ and $\{c_{kj}\}$ are complex, and the powers of polynomials, $\{b_{kj}\}$ and

$\{d_{kj}\}$, are assumed to be real numbers. DFT is a special solution of GDFT where $\varphi_k(n) = a_{k1} = k$,

$a_{k2} = a_{k3} = \dots = a_{kN} = 0$, and $b_{k1} = b_{k2} = \dots = b_{kN} = 0$ in (10) and (11), for all k .

Note that several authors also have used the term ‘‘Generalized DFT’’ in the literature prior to this work. However, their work was linear phase extensions of DFT [24-28] and special cases of the GDFT.

III. DESIGN OF OPTIMAL PHASE FOR MINIMIZED CORRELATIONS

We present a GDFT design method in this section, show its efficiency and merit through several practical examples. This method is built as an enhancement to DFT due to its wide use and fast implementations.

Therefore, simple modifications to the celebrated fast Fourier transform (FFT) algorithms offer promising fast GDFT (FGDFT) techniques to be used in future technologies.

DFT matrix of size $N \times N$ is defined as

$$A_{DFT} = [A_{DFT_{k,n}}] = [e^{j(2\pi/N)kn}] \quad (12)$$

$$k, n = 0, 1, 2, \dots, N-1$$

GDFT is designed to enhance the traditional DFT based on a performance metric related to the application of interest. Therefore, we write the GDFT matrix as a product of three orthogonal matrices

$$\begin{aligned}
A_{GDFT} &= G_1 A_{DFT} G_2 \\
A_{GDFT} A_{GDFT}^{-1} &= I \\
A_{GDFT}^{-1} &= A_{GDFT}^{*T} \\
G_1 G_1^{*T} &= I \quad G_2 G_2^{*T} = I
\end{aligned} \tag{13}$$

where diagonal matrices G_1 and G_2 are defined as

$$G_1(k,n) = \left\{ \begin{array}{ll} e^{j\theta_{kk}} & k = n \\ 0 & k \neq n \end{array} \right\} \quad k,n = 0,1,\dots,N-1 \tag{14.a}$$

and

$$G_2(k,n) = \left\{ \begin{array}{ll} e^{j\gamma_{mm}} & k = n \\ 0 & k \neq n \end{array} \right\} \quad k,n = 0,1,\dots,N-1 \tag{14.b}$$

The notation $(*T)$ indicates conjugate and transpose operations applied to the matrix, and I is the *identity matrix*. $G_1 = I$ and $G_2 = G$ is considered in this paper. Therefore, GDFT matrix becomes

$$A_{GDFT} = A_{DFT} G \tag{15}$$

Note that the elements of diagonal matrices G_1 and G_2 in (14) might also be defined as non-constant modulus for additional design flexibilities to further improvements.

A. Design Metrics:

Several correlation metrics are known in the literature. They mostly depend on *aperiodic correlation functions (ACF)* of the spreading code set. The ACF, $\{d_{k,l}(m)\}$, of a set $\{e_k(n)\}$ is defined as [16],

$$d_{k,l}(m) = \begin{cases} \frac{1}{N} \sum_{n=0}^{N-1-m} e_k(n) e_l^*(n+m), & 0 < m \leq N-1 \\ \frac{1}{N} \sum_{n=0}^{N-1+m} e_k(n-m) e_l^*(n), & 1-N < m \leq 0 \\ 0, & |m| \geq N \end{cases}; \quad 0 < k, l \leq N-1 \quad (16)$$

Out-of-phase autocorrelation sequence of the complex sequence $e_k(n)$ is also defined from (16) as the absolute sequence $|d_{k,k}(m)|$. Similarly, out-of-phase cross-correlation of two complex sequences $e_k(n)$ and $e_l(n)$ is defined as the absolute function $|d_{k,l}(m)|$.

Various correlation metrics are defined below and used in optimal phase design for GDFT examples given in the paper where M is the size of the set, and N is the length of codes.

- a. Maximum value of out-of-phase auto-correlation, d_{am} :

$$d_{am} = \max_{\substack{0 \leq k < M \\ 1 \leq m < N}} \{|d_{k,k}(m)|\} \quad (17)$$

- b. Maximum value of out-of-phase cross-correlation, d_{cm} :

$$d_{cm} = \max_{\substack{0 \leq k, l < M \\ 0 \leq m < N \\ k \neq l}} \{|d_{k,l}(m)|\} \quad (18)$$

$$d_{\max} = \max \{d_{am}, d_{cm}\} \quad (19)$$

The relationship between d_{am} and d_{cm} was derived by Sarwate in [17],

$$(2N-1)d_{cm}^2 + \frac{(2N-1)}{(M-1)}d_{am}^2 \geq 1 \quad (20)$$

This leads us to the Welch bound for complex spreading sequences defined as [18],

$$d_{\max} = \max \{d_{am}, d_{cm}\} = \sqrt{\frac{M-1}{M(2N-1)-1}} \quad (21)$$

- c. Mean square value of auto-correlation sequences of a set, R_{AC} :

$$R_{AC} = \frac{1}{M} \sum_{k=1}^M \sum_{\substack{m=1-N \\ m \neq 0}}^{N-1} |d_{k,k}(m)|^2 \quad (22)$$

d. Mean square value of pair-wise cross-correlation sequences of a set, R_{CC} :

$$R_{CC} = \frac{1}{M(M-1)} \sum_{k=1}^M \sum_{\substack{l=1 \\ l \neq k}}^M \sum_{m=1-N}^{N-1} |d_{k,l}(m)|^2 \quad (23)$$

e. The merit factor F_k of the k^{th} code of a set [19]

$$F_k = \frac{d_{k,k}(0)}{2 \sum_{m=1}^{N-1} |d_{k,k}(m)|^2} \quad (24)$$

Although we did not present the merit factors of designed codes in this paper, large values of F_k are desired in CDMA communications systems in order to improve the code synchronization and amiability [19].

B. Design of Optimal Phase:

A cost function formulated by these metrics for a GDFT set of M sequences of length-N is written as

$$C_{N,M} = \alpha \sum_{k=0}^{M-1} F_k - \beta d_{am} - \delta d_{cm} - \eta R_{AC} - \gamma R_{CC} \quad (25)$$

where $\{\alpha, \beta, \delta, \eta, \gamma\}$ are the weighting coefficients. One might set the values of these coefficients according to the application at hand. As an example, assume that the system is a multi-user DS/CDMA system operating in a multi-path free environment and the transmitter and the receiver of the intended user are perfectly matched (synchronized). In this scenario, the only source of interference is the other users co-exist in the system and quantified in the terms d_{cm} and R_{CC} in (25). Thus, for this system the weighting coefficients $\{\alpha, \eta, \beta\}$ in (25) are set to zero since they have no impact on the performance metrics of interest. The values of $\{\delta, \gamma\}$ are set according to the application scenario under consideration.

We focus on the design of optimal phase shaping function, $\psi(n)$, defined below based on a defined metric. Note that the phase function of the k^{th} basis function as given (9), $\{\varphi_k(n) n\}$, is now decomposed into two time functions where $\psi(n)$ represents the non-linear component as written in

$$\begin{aligned}\hat{\varphi}_k(n) &= \varphi_k(n)n = kn + \psi(n) \text{ for } k = 0, 1, \dots, N-1 \text{ and } n = 1, \dots, N-1 \\ \psi(n) &= \hat{\varphi}_k(n) - kn = [\varphi_k(n) - k]n \text{ for } k = 0, 1, \dots, N-1 \text{ and } n = 1, \dots, N-1 \\ \psi(0) &\in \mathbb{R} \quad \hat{\varphi}_k(0) = \psi(0)\end{aligned}\tag{26}$$

The linear term in (26) is highlighted due to its significance in the orthogonality requirements of (7). The GDFT framework offers the mathematical freedom to define the non-linear phase shaping function $\psi(n)$ of a set regardless of its orthogonality requirements for the optimal design. Note that any $\psi(n)$ function of (26) will give us an orthogonal GDFT, and therefore, it is an uncountable set.

The pair-wise cross-correlation sequence of GDFT *basis function pair* $\{e_k(n), e_l(n)\}$ with length N is defined as

$$R_{\hat{\varphi}_k \hat{\varphi}_l}(m) = \sum_{n=0}^{N-1} e^{j(\frac{2\pi}{N})\hat{\varphi}_k(n)} e^{-j(\frac{2\pi}{N})\hat{\varphi}_l(n+m)} = \sum_{n=0}^{N-1} e^{j(\frac{2\pi}{N})[-lm+(k-l)n+\psi(n)-\psi(n+m)]}\tag{27}$$

where $R_{\hat{\varphi}_k \hat{\varphi}_l}(m) = 0; \forall m$ for the ideal case, and $R_{\hat{\varphi}_k \hat{\varphi}_l}(0) = 0$ implies the orthogonality of the pair.

Similarly, one can define the auto-correlation function of a GDFT basis function as written

$$R_{\hat{\varphi}_k \hat{\varphi}_k}(m) = \sum_{n=0}^{N-1} e^{j(\frac{2\pi}{N})\hat{\varphi}_k(n)} e^{-j(\frac{2\pi}{N})\hat{\varphi}_k(n+m)} = \sum_{n=0}^{N-1} e^{j(\frac{2\pi}{N})[-km+\psi(n)-\psi(n+m)]}\tag{28}$$

where $R_{\hat{\varphi}_k \hat{\varphi}_k}(m) = \delta(m)$ for the ideal case. The correlation sequence of a basis pair is incorporated in

R_{AC} and R_{CC} metrics of (22) and (23), respectively, in the following design example.

Since there is not a general closed form expression for $\psi(n)$, we used the numerical design tools in Mathematica and MATLAB software in order to design its optimal by minimizing the correlation

metrics of (22) and (23). Note that the entire set uses the same phase shaping function, and there are

$P_N = \binom{N}{2} = \frac{N!}{(N-2)!2!}$ basis function pairs in a set of size N to be simultaneously considered in the design.

C. A Closed Form Phase Shaping Function:

Let's keep only the first two terms in (11) and replace the rest with zero as follows

$$\begin{aligned} \varphi_k(n) &= a_{k1}n^{b_{k1}} + a_{k2}n^{b_{k2}} \\ a_{k1} &= k, \quad b_{k1} = 0 \\ \varphi_k(n) &= k + a_{k2}n^{b_{k2}} \end{aligned} \quad (29)$$

Hence, the GDFT basis functions are expressed as

$$e_k(n) = e^{j(2\pi/N)\varphi_k(n)n} = e^{j(2\pi/N)kn} e^{j(2\pi/N)[a_{k2}n^{(b_{k2}+1)}]} \quad k, n = 0, 1, \dots, N-1 \quad (30)$$

The first exponential term in (30) is the DFT kernel with linear phase, and the second one defines the elements of G matrix in phase shaping function,

$$\psi(n) = a_{k2}n^{(b_{k2}+1)} \quad n = 0, 1, \dots, N-1, \quad (31)$$

and $\{e_k(n)\}$ are the row sequences of A_{GDFT} matrix as written in (12). In this representation, varying the

values of a_{k2} and b_{k2} generates a medley of GDFT sets along with their associated nonlinear phase functions yielding the corresponding auto- and cross-correlations. This suggests that a brute force search algorithm scans the phase space for various search grid resolutions to find optimum G matrices with respect to the given design metric where $\psi(n) \in [0, 2\pi]; \forall n$. The resolution of the search algorithm is

defined by the number of bits representing each phase value. For m bits, the phase search resolution is calculated as $\Delta\theta = \frac{2\pi}{2^m}$, and $m=5$ is picked in the search process for this example. The optimal phase

shaping function of (26) obtained from brute force search is approximated by a closed form expression

using a curve-fitting technique in the software tool called Table Curve 2D. The fitted phase shaping function to the brute force search with minimized d_{cm} for size $N=8$ is expressed as

$$\psi(n) = a_1 \exp\left(-\left[\frac{n-b_1}{c_1}\right]^2\right) + a_2 \exp\left(-\left[\frac{n-b_2}{c_2}\right]^2\right) \quad n = 0, 1, \dots, N-1 \quad (32)$$

It is a second degree *Gaussian function* defined with six parameters $\{a_1, b_1, c_1, a_2, b_2, c_2\}$. The values of the parameter set, $\{a_1, b_1, c_1, a_2, b_2, c_2\}$ are chosen for the best fit employing an error criterion. Note that for this optimization, the cost function of (25) is defined as

$$C_{N,M} = d_{cm} \quad (33)$$

where $\delta = -1, \alpha = \beta = \eta = \gamma = 0$.

The phase shaping function defined in (32) will be used for code basis generation in this paper. The numerical optimization tool, *fminsearch* of MATLAB is utilized to obtain *PSF*'s for the optimum GDFT sets obtained with respect to various cost functions and sizes. The closed form phase shaping function of (32) is plugged in the phase function of (26). Figure 1 displays the resulting $\psi(n)$ that approximates the brute force based GDFT design minimizing d_{cm} metric with the parameter values of $\{a_1 = 1, b_1 = 1.75, c_1 = 3.75, a_2 = 1.75, b_2 = 6, c_2 = 0.5\}$ in (32) for $N=8$.

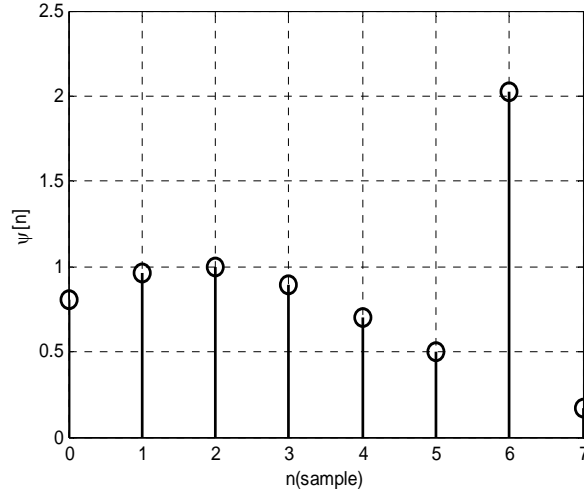


Figure 1. Closed form phase shaping function $\psi(n)$ of (32) approximating to brute force search based optimal solution with minimized d_{cm} and $N = 8$.

Similarly, the parameter sets of closed form phase shaping functions approximating to brute force based optimal solutions for various correlation metrics, e.g. d_{cm} and R_{AC} , and sizes are tabulated in Table I. Although some parameter values in Table II are high, the phase functions of GDFT are periodic and constrained to be within the range of $-\pi$ to $+\pi$.

R_{AC} and d_{cm} performance of GDFT and DFT for $N=128$ are compared in Figure 2.A and Figure 2.B, respectively. In the cross-correlation figures, only the first pair of a set is considered since it generates the highest cross-correlations for both GDFT and DFT. Our studies have shown that the closed form phase shaping function defined in (32) approximates well to brute force search based optimal solutions and provides low values of d_{cm} , R_{AC} , d_{am} and R_{CC} regardless of the size N .

TABLE I

Parameter values of the closed form phase shaping function $\psi(n)$ defined in (31) for various sizes.

Size (N)	$\{a_1, b_1, c_1, a_2, b_2, c_2\}$
----------	------------------------------------

	d_{cm}	R_{AC}
8	{1, 1.75, 3.75, 1.75, 6, 0.5}	{-1.13, 5.03, 0.18, 6.35, 1.83, 1.3}
16	{ 5.108, 1.9432, 0.3797, 11.1226, 6.2617, 33.1041}	{59.9669, 0.516, 8.6189, 127.9627, 11.7657, 11.8332}
32	{1.7623, -0.01383, 23.2082, 24.4758, 25.7258, 0.7161}	{223.257, 4.4965, 0.2227, 2308.2868, 18.023, 66.299}
64	{-26.6962, 8.4073, 155.099, 51.3974, 43.4337, 1.9759}	{17.4042, 4.7358, 0.1745, 6419.2508, 36.1610, 109.4535}
128	{0.9451, -0.0352, 436.0006, 118.182, 36.1617, 4.1372}	{-291014.6087, -14297.5518, 16446.8926, 534786.2823, 58.6139, 1031.3806}

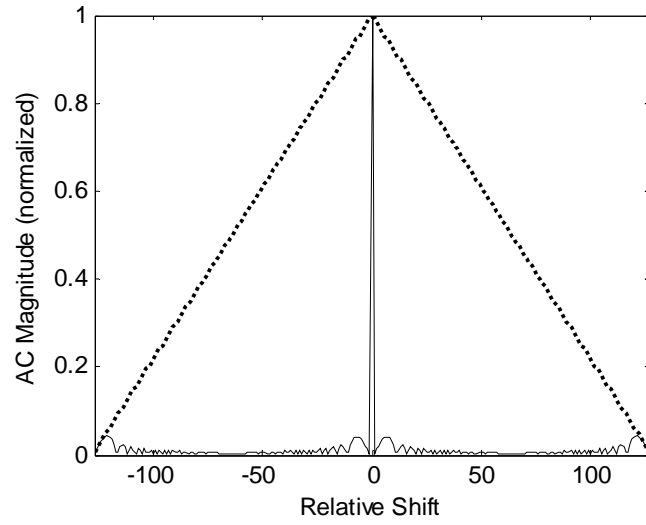


Figure 2.A Magnitude of auto-correlation functions for minimized- R_{AC} based GDFT (solid line) and DFT (dashed line) with $N=128$.

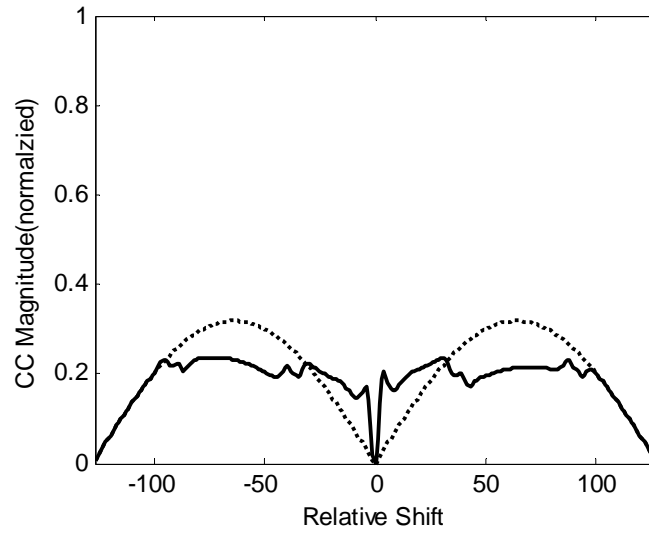


Figure 2.B Magnitude of cross-correlation functions for minimized- d_{cm} based GDFT (solid line) and DFT (dashed line) with $N=128$.

TABLE II.A

Values of correlation metrics for minimized d_{cm} based GDFT and DFT with sizes $N=8, 16, 32, 64, 128$.

Size (N)	Correlation metrics for minimized d_{cm} based GDFT and DFT				
	d_{am}	d_{cm}	d_{max}	R_{AC}	R_{CC}
8 GDFT	0.703	0.288	0.703	3.261	0.534
8 DFT	0.875	0.327	0.875	4.375	0.375
16 GDFT	0.764	0.267	0.764	6.918	0.539
16 DFT	0.938	0.321	0.938	9.688	0.354
32 GDFT	0.827	0.251	0.827	14.357	0.536
32 DFT	0.969	0.319	0.969	20.34	0.344
64 GDFT	0.894	0.243	0.894	25.61	0.593
64 DFT	0.984	0.318	0.984	41.67	0.339
128 GDFT	0.956	0.236	0.956	53.49	0.579
128 DFT	0.992	0.318	0.992	84.33	0.335

TABLE II.B

Values of correlation metrics for minimized R_{AC} based GDFT and DFT with sizes $N=8, 16, 32, 64, 128$.

Size (N)	Correlation metrics for minimized R_{AC} based GDFT and DFT
----------	---

	d_{am}	d_{cm}	d_{max}	R_{AC}	R_{CC}
8 GDFT	0.125	0.679	0.679	0.089	0.987
8 DFT	0.875	0.327	0.875	4.375	0.375
16 GDFT	0.137	0.935	0.935	0.136	0.991
16 DFT	0.938	0.321	0.938	9.688	0.354
32 GDFT	0.083	0.966	0.966	0.105	0.997
32 DFT	0.969	0.319	0.969	20.34	0.344
64 GDFT	0.071	0.982	0.998	0.092	0.998
64 DFT	0.984	0.318	0.984	41.67	0.339
128 GDFT	0.044	0.992	0.992	0.056	0.999
128 DFT	0.992	0.318	0.992	84.34	0.336

Tables II.A and II.B compare the correlations of GDFT and DFT for sizes $N=8, 16, 32, 64, 128$.

Similarly, Table III compares correlation performance of various known constant modulus codes for the length of $N=64$ ($61/63$). These performance results depict the benefits of employing nonlinear phase GDFT over linear phase DFT in applications where correlations are of importance in the system performance.

TABLE III

Values of correlation metrics for various code families with comparable sizes, $N=61, 63$ or 64 .

Code	d_{am}	d_{cm}	d_{max}	R_{AC}	R_{CC}
Walsh [64x64]	0.984	0.984	0.984	10.391	0.835
DFT [64x64]	0.984	0.318	0.984	41.67	0.339
63/64 Gold	0.349	0.349	0.349	0.995	0.984
61/60 Oppermann $\{m, n, p\} = \{1, 1.15, 1\}$ [9]	0.984	0.371	0.984	39.24	0.346
GDFT [64x64] ($opt d_{cm}$)	0.894	0.243	0.894	25.61	0.593
GDFT [64x64] ($opt R_{AC}$)	0.071	0.982	0.998	0.092	0.998

The minimizations of auto- and cross-correlation functions of an orthogonal set have conflicting requirements in the time-frequency plane dictated by the uncertainty principle [20]. Therefore, the

interdependence of the auto- and cross-correlation metrics R_{AC} and R_{CC} , respectively, are jointly expressed in [21]

$$R_{CC}(M-1) + R_{AC} \geq M-1 \quad (34)$$

In OFDM communications systems, frequency localization is more important and the optimization on R_{CC} parameters is emphasized. In contrast, in a DS/CDMA communications system, both R_{AC} and R_{CC} are equally significant. The low values of R_{AC} is desirable for synchronization of the system and spreading of code spectra; and the low values of R_{CC} is required to minimize multi-user interference (MUI) of a correlation based detector defining BER performance of the system.

In the following section, the proposed GDFT codes are employed in a DS/CDMA communications system where the correlations play a crucial role in BER performance.

IV. BER PERFORMANCE OF DS/CDMA COMMUNICATIONS SYSTEMS USING VARIOUS CONSTANT MODULUS CODES

Each user is assigned a unique orthogonal spreading code in Direct Sequence-CDMA (DS/CDMA) based multi-user communications systems. In Additive White Gaussian Noise (AWGN) downlink channels, orthogonality of codes is necessary and sufficient to cancel inter-user interference due to the synchronous nature of communications. In contrast, non-zero cross-correlations of delayed spreading codes degrade BER performance of the system.

Assume that $b_k(t)$ is the data sequence represented in continuous time for the k^{th} user, and $e_k(t)$ is the resulting spreading code waveform as expressed [16]

$$\begin{aligned} b_k(t) &= \sum_{l=-\infty}^{\infty} b_{k,l} p_T(t-lT) \\ e_k(t) &= \sum_{m=-\infty}^{\infty} e_k(m) p_{T_c}(t-mT_c) \end{aligned} \quad (35)$$

where $b_{k,l} \in \{+1, -1\}$, $p_\tau(t) = 1$ for $0 \leq t \leq \tau$, otherwise $p_\tau(t) = 0$. T is the symbol duration and T_c is the chip duration.

The received signal in a synchronous channel (downlink) is written as [16]

$$r(t) = n(t) + \sum_{k=0}^{K-1} A_k e_k(t) b_k(t) \quad (36)$$

where K is the number of users in the channel, A_k is the received amplitude due to the k^{th} user in the channel, and $n(t)$ is the channel noise and assumed to be Gaussian with spectral density function of $N_0 / 2$. In a power-controlled system, A_k is assumed to be unity for all users. Similarly, for asynchronous communications of uplink channel with $A_k = 1$ (36) is re-written as follows

$$r(t) = n(t) + \sum_{k=0}^{K-1} A_k e_k(t - \tau_k) b_k(t - \tau_k) \quad (37)$$

where τ_k is the channel delay for k^{th} user. If a match filter for the l^{th} user's spreading code, $e_l(t)$, is used in the receiver, the filter output at $t = T$ is given by [16]

$$Z_l = \left\{ b_{l,0} + \sum_{\substack{k=1 \\ k \neq l}}^{K-1} [b_{k,-1} R_{k,l}(\tau_k) + b_{k,0} \hat{R}_{k,l}(\tau_k)] \right\} + \int_0^T n(t) e_l(t) dt \quad (38)$$

where $b_{l,0}$ is l^{th} user's transmitted data in the first symbol interval that is to be detected in the receiver. The continuous-time partial correlation functions, $R_{k,l}(\tau)$ and $\hat{R}_{k,l}(\tau)$ are defined as

$$\begin{aligned} R_{k,l}(\tau) &= \int_0^\tau e_k(t - \tau) e_l(t) dt \\ \hat{R}_{k,l}(\tau) &= \int_\tau^T e_k(t - \tau) e_l(t) dt \end{aligned} \quad (39)$$

for $0 \leq \tau \leq T$. In Equation (38), the second term in the parenthesis is interference due to $K-1$ users in the system, and it is called multi-user interference (MUI). In order to increase detection

probability of the intended user bits, this term is to be minimized. In other words, $R_{k,l}(\tau)$ and $\hat{R}_{k,l}(\tau)$ should be minimized for performance improvements. In [16], Pursley showed that for the interval $0 \leq jT_c \leq \tau \leq (j+1)T_c$ where j is the chip index of a symbol, the partial cross-correlations can be defined in terms of ACF as follows

$$\begin{aligned} R_{k,l}(\tau) &= d_{k,l}(j-N)T_c + [d_{k,l}(j+1-N) - d_{k,l}(j-N)](\tau - jT_c) \\ \hat{R}_{k,l}(\tau) &= d_{k,l}(j)T_c + [d_{k,l}(j+1) - d_{k,l}(j)](\tau - jT_c). \end{aligned} \quad (40)$$

In the case of frequency selective (multi-path) channel, this analysis is valid with the change in the channel characteristic function defined as follows. An L -tap frequency selective channel for the k^{th} user is expressed as [22]

$$h_k(t) = \sum_{m_k=0}^{L_k} \beta_{k,m_k} \delta(t - \tau_{k,m_k}) \quad (41)$$

where L_k is the number of multipath components of channel for user k , β_{k,m_k} is the amplitude of each path, that is a Rayleigh distributed random variable. Therefore, the received signal of this scenario becomes

$$r(t) = n(t) + \sum_{k=0}^{K-1} \sum_{m_k=1}^{L_k} \beta_{k,m_k} e_k(t - \tau_{k,m_k}) b_k(t - \tau_{k,m_k}) \quad (42)$$

The output of the correlator at the l^{th} receiver is written as

$$r(t) = b_{l,0} \beta_{l,0} + \int_0^T n(t) e_l(t - \tau_{l,0}) dt + \sum_{k=0}^{K-1} \sum_{m_k=1}^{L_k} \alpha_{k,m_k} \quad (43)$$

The third term in (43) is the interference due to other $K-1$ active users in the channel along with the delayed (faded) versions of these user codes, and the delayed versions of the intended user's own code.

This analysis is presented for real spreading codes due to its ease. Interested readers are referred to [16] [22], [23] for more detailed treatment and also for complex spreading codes.

We present BER curves of the proposed codes along with other families employed in DS/CDMA communications systems for performance comparisons. The relationship between the correlation metrics and BER performance is highlighted for various scenarios considered in the following sections.

A. Asynchronous AWGN Channel

Figure 3 displays BER performances of various GDFT sets of size 8 optimized on correlation metrics d_{cm} , d_{max} , R_{AC} and R_{CC} for an asynchronous AWGN channel with two users. It is observed from the curves that GDFT set optimized with respect to d_{cm} metric provides superior performance than other optimized solutions for this case.

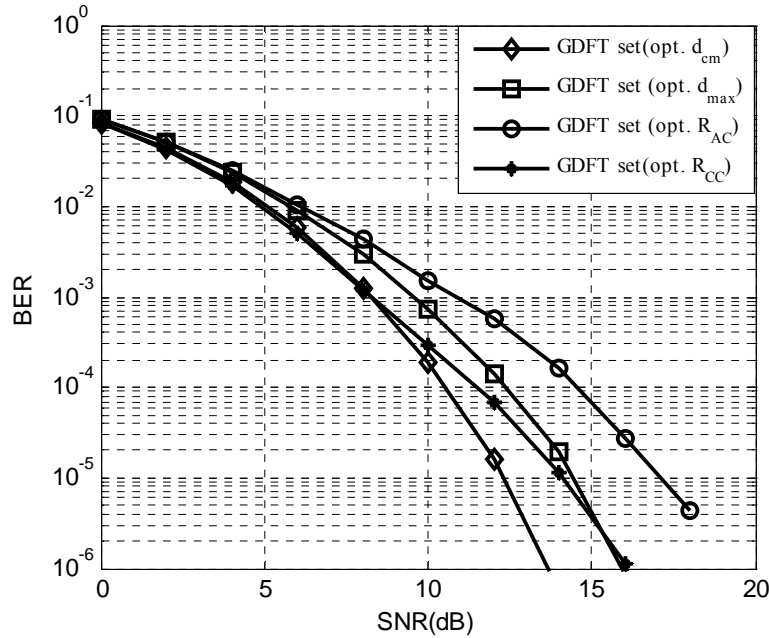


Figure 3 BER performance of GDFT sets optimized based on various correlation metrics for an asynchronous AWGN channel with two users and code size of $N=8$.

Similarly, Figure 4 compares the BER performances of GDFT sets minimizing d_{cm} with various lengths. The performance improves as the spreading code length increases in DS/CDMA systems as expected.

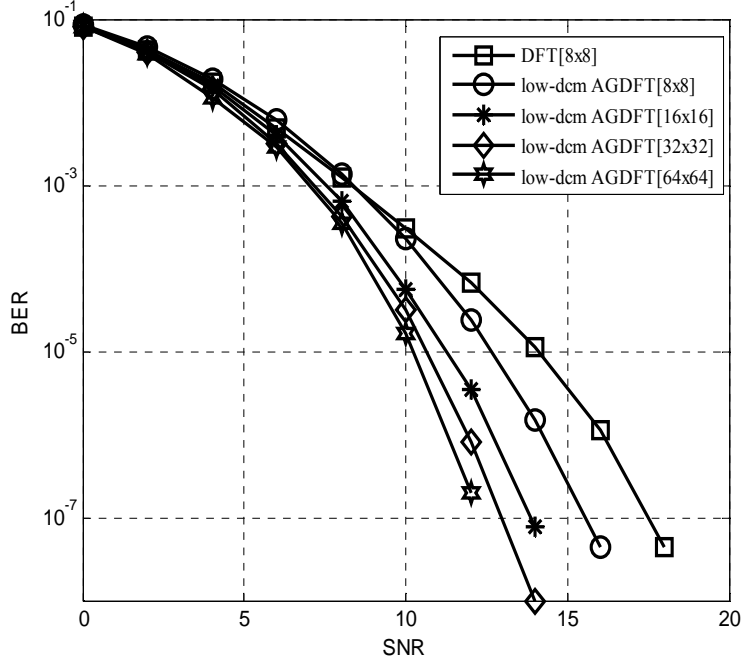


Figure 4 BER performances of various optimal GDFT sets in an asynchronous AWGN channel of a two-user communications system with code lengths $N=8, 16, 32,$ and 64 .

Figure 5 displays superior performance of GDFT over the competing code families under the same test conditions. The improved correlation of GDFT manifests itself in improved BER performance in multi-user communications systems considered in the paper.

B. Synchronous Rayleigh Channel

We performed similar BER performance simulations for a Rayleigh channel model. A two-ray multipath channel is expressed in (41) with $L_k = 1$ for all users. The parameters $\beta_{k,0}$ and $\beta_{k,1}$ are

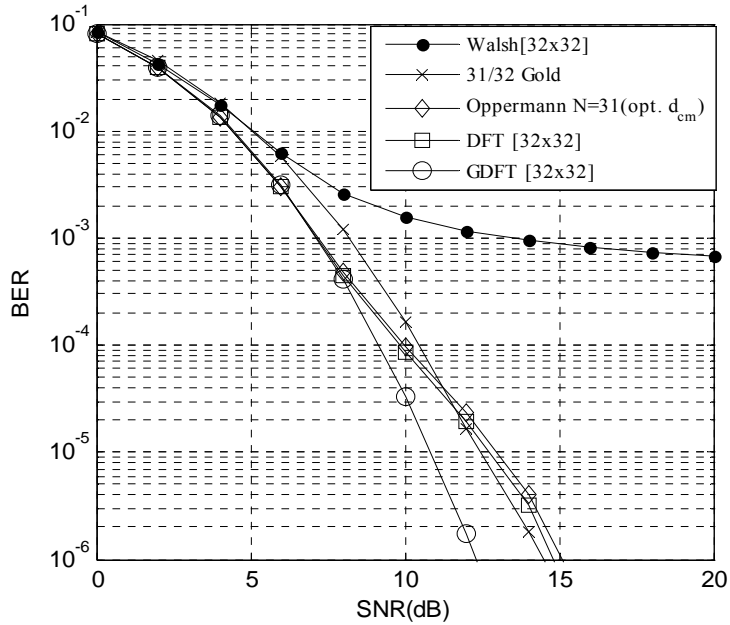


Figure 5 BER performances of several competing code families in asynchronous AWGN channel of a two-user DS/CDMA communications system for length $N=32$ ($N=31$ for Gold and Oppermann codes).

the Rayleigh distributed random variables defining power of the desired and interfering paths, respectively, and the sum of $\beta_{k,0}$ and $\beta_{k,1}$ is normalized to one. Figure 6 displays BER performance of size-8 GDFT sets optimized on various correlation metrics for single user in a Rayleigh multipath channel when the power of interfering path is 3dB less than the power of the desired path ($D/I = 3dB$) with the corresponding time delays, $\tau_{k,0} = 0$ and $\tau_{k,1} = T/8$, respectively. From the BER curves, it is observed that the best performance is achieved when the GDFT set is optimized based on R_{AC} in this case. Therefore, the GDFT is optimized with respect to R_{AC} in the examples given next.

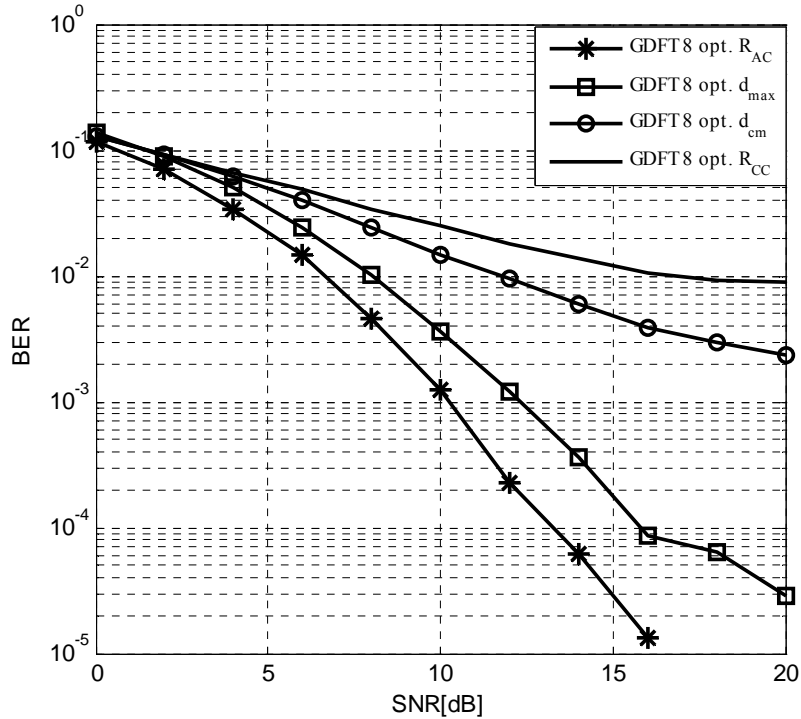


Figure IV BER performance of GDFT sets optimized on various correlation metrics for a single user case in a two-ray Rayleigh multi-path channel model of (40).

Figure 7 displays BER performance of two-users in synchronous Rayleigh multipath channel when the power of interfering path is 5dB less than the power of the desired path with the corresponding delays, $\tau_{k,0} = 0$ and $\tau_{k,1} = T/8$, respectively. The performance of a single user AWGN channel is also included in the figure as the upper performance bound. GDFT set for this simulation is generated by optimal design of PSF defined in (32) based on R_{AC} of (22).

From the figure, one might conclude that DFT set with intrinsic high R_{AC} values yields a poor BER performance even for single user case. The GDFT sets with their superior R_{AC} values significantly outperform DFT sets for all the code lengths considered. In contrast, note that the BER performance gets worse when the number of users in the multiuser communications system is increased due to the increasing significance of code cross correlations. We highlight from the BER simulations that MUI for

two-users case is strongly coupled with the correlation metric d_{cm} whereas ISI for the same communications scenario is coupled with R_{AC} . In a multiuser communications system, depending on the dominant factor, one may employ the most advantageous GDFT set optimized on any correlation metric, namely d_{cm} , R_{AC} , d_{am} , R_{CC} or F_k . Although, we limited our BER simulations to GDFT sets optimized only for one correlation metric at a time, optimal designs can easily be extended to joint optimization problem of multiple metrics as stated in (25).

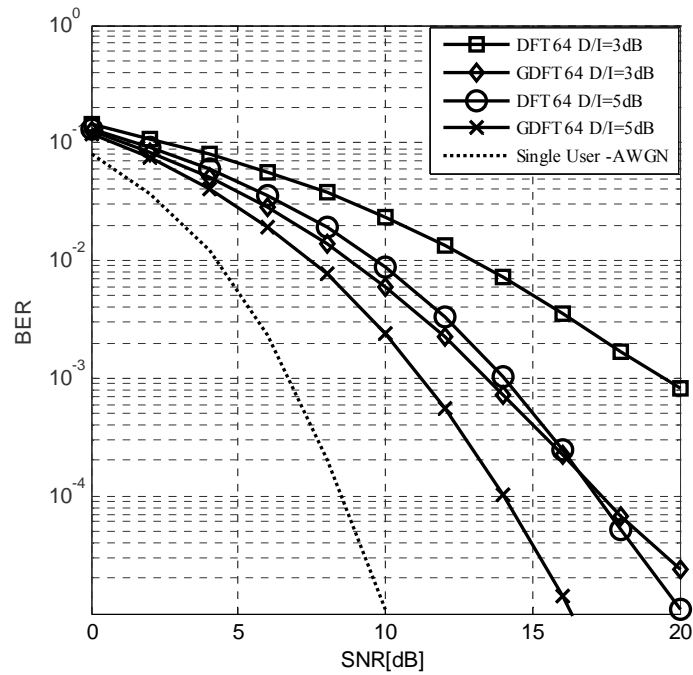


Figure 7 BER Performance of length 64 DFT and GDFT spreading code sets over Rayleigh fading channels for a single user and synchronous two-user cases with $D/I = 5dB$.

V. CONCLUSIONS

In this paper, we presented GDFT with nonlinear phase to design constant modulus orthogonal set with superior correlations compared to its linear phase antecedents. We showed the significance of phase shaping function in order to improve the auto- and cross-correlations of a code set and forwarded several optimal design methods. Then, we displayed the improved BER performance of GDFT codes in a

DS/CDMA communications system, and compared with various known code families employed under the same test conditions. It is concluded that the nonlinearity of phase functions in GDFT is a marked departure from the traditional linear phase DFT, and the first offers a flexible mathematical tool to design constant modulus sets with the desired time and frequency domain characteristics. We expect the future communications systems, spanning from CDMA to OFDM types, and other engineering applications currently using DFT might benefit from the GDFT framework.

REFERENCES

- [1] R. Gold, "Optimal Binary Sequences for Spread Spectrum Multiplexing," IEEE Trans. on Info. Theory, pp. 619-621, Oct. 1967.
- [2] K. Fazel and S. Kaiser, Multi-carrier and Spread Spectrum Systems. Wiley 2003.
- [3] J. L. Walsh, "A Closed Set of Normal Orthogonal Functions," American Journal of Mathematics, vol. 55, pp. 5-24, 1923.
- [4] A.N. Akansu and R. Poluri, "Walsh-like Nonlinear Phase Orthogonal Codes for Direct Sequence CDMA Communications," IEEE Trans. on Signal Processing, pp. 3800-3806, July 2007.
- [5] R.L. Frank, S.A. Zadoff and R. Heimiller, "Phase Shift Pulse Codes with Good Periodic Correlation Properties," IRE Trans. on Information Theory, vol. IT-8, pp. 381-382, 1962.
- [6] R.L. Frank, "Polyphase Codes with Good Non-periodic Correlation Properties," IEEE Trans. on Info. Theory, vol. IT-9, pp. 43-45, 1963.
- [7] D.C. Chu, "Polyphase Codes with Good Periodic Correlation Properties," IEEE Trans. on Information Theory, pp. 720-724, July 1972.
- [8] I. Oppermann and B.S. Vucetic, "Complex Valued Spreading Sequences with A Wide Range of Correlation Properties," IEEE Trans. on Communications, vol. 45, pp. 365-375, March 1997.
- [9] I. Oppermann, "Orthogonal Complex-valued Spreading Sequences with A Wide Range of Correlation Properties," IEEE Trans. on Communications, vol. 45, pp. 1379-1380, Nov. 1997.

- [10] A.N. Akansu and H. Agirman-Tosun, "Generalized Discrete Fourier Transform: Theory and Design Methods," Proc. IEEE Sarnoff Symposium, March 2009.
- [11] A.N. Akansu and H. Agirman-Tosun, "Improved Correlation of Generalized Discrete Fourier Transform with Nonlinear Phase for OFDM and CDMA Communications," Proc. EUSIPCO European Signal Processing Conference, Aug. 2009.
- [12] A.N. Akansu and H. Agirman-Tosun, "Generalized Discrete Fourier Transform with Optimum Correlations," Proc. IEEE ICASSP, March 2010.
- [13] K. Ireland and M. Rosen, *A Classical Introduction to Modern Number Theory*. Springer-Verlag, 1993.
- [14] W. Narkiewicz, *Elementary and Analytic Theory of Numbers*. Springer-Verlag, 1990.
- [15] A. Papoulis, *Signal Analysis*. McGraw-Hill, 1977.
- [16] D. Sarwate, M. Pursley, W. Stark, "Error Probability for Direct-Sequence Spread-Spectrum Multiple-Access Communications-Part I: Upper and Lower Bounds," *IEEE Trans. on Communications*, vol. 30, pp. 975-984, May 1982.
- [17] D. Sarwate, "Bounds on Crosscorrelation and Autocorrelation of Sequences," *IEEE Trans. on Info. Theory*, vol. 25, pp. 724-725, November 1979.
- [18] L. Welch, "Lower Bounds on the Maximum Cross Correlation of Signals," *IEEE Trans. on Info. Theory*, vol. 20, pp. 397-399, May 1974.
- [19] M. Golay, "The Merit Factor of Long Low Autocorrelation Binary Sequences," *IEEE Transactions on Information Theory*, vol. 28, no. 3, pp. 543-549, 1982.
- [20] A.N. Akansu and R.A. Haddad, *Multiresolution Signal Decomposition: Transforms, Subbands and Wavelets*, 2nd Edition. Elsevier, 2001.
- [21] B. Natarajan, S. Das and D. Stevens, "Design of Optimal Complex Spreading Codes for DS-CDMA Using an Evolutionary Approach," Proc. IEEE Globecom, vol. 6, pp. 3882-3886, 2004.
- [22] J. Cheng, and N. Beaulieu, "Accurate DS-CDMA Bit-error Probability Calculation in Rayleigh Fading," *IEEE Transactions on Wireless Communications*, vol. 1, no. 1, pp. 3-15, 2002.

- [23] A.W. Lam, F.M. Ozluturk, "Performance Bounds for DS/SSMA communications with complex signature sequences," IEEE Transactions on Communications, vol. 40, no. 10, pp.1607-1614, Oct. 1992.
- [24] G. Bongiovanni, P. Corsini and G. Frosini, "One-dimensional and Two-dimensional Generalized Discrete Fourier Transform," IEEE Trans. Acoust. Speech Signal Process. Vol. ASSP-24, pp. 97-99, Feb. 1976.
- [25] P. Corsini and G. Frosini, "Properties of the Multidimensional Generalized Discrete Fourier Transform," IEEE Trans. on Computers, C-28, pp. 819-830, Nov. 1979.
- [26] L. Rinaldi and P.E. Ricci, "Complex Symmetric Functions and Generalized Discrete Fourier Transform," Rendiconti del Circolo Matematico di Palermo, vol. 45, no. 1, Jan. 1996. (Online: <http://www.springerlink.com/content/6310t2352461n4u1/>)
- [27] E. Stade and E.G. Layton, "Generalized Discrete Fourier Transforms: The Discrete Fourier-Riccati-Bessel Transform," Computer Physics Communications, vol. 85, pp. 336-370, March 1995.
- [28] V. Britanak and K.R. Rao, "The Fast Generalized Discrete Fourier Transforms: A Unified Approach to The Discrete Sinusoidal Transforms Computation," Signal Processing, vol. 79, pp. 135-150, Dec. 1999.